eLIFE elifesciences.org

RESEARCH ARTICLE

Figures and figure supplements

Regulation of zebrafish melanocyte development by ligand-dependent BMP signaling

Alec K Gramann *et al*

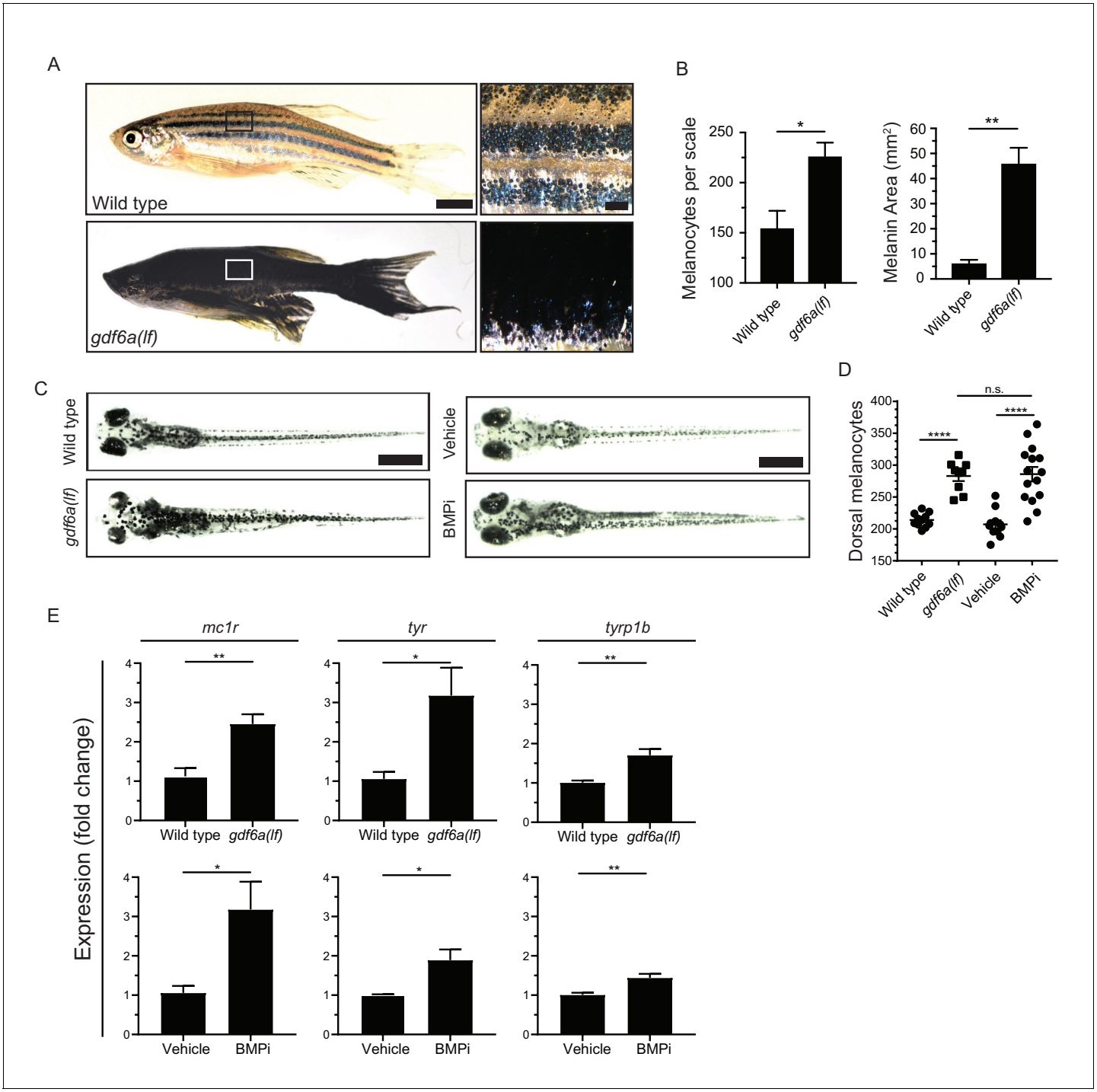

Figure 1. *gdf6a* loss or BMP inhibition causes the development of supernumerary melanocytes. (**A**) Images of wild-type and *gdf6a(lf)* adult zebrafish, scale bar = 4 mm, inset scale bar = 1 mm. (**B**) Quantification of number of melanocytes (left) and scale pigmentation using melanin coverage (right), n = 3 scales per group. (**C**) Wild-type and *gdf6a(lf)* embryos imaged at 5 days post fertilization (DPF); vehicle- and BMPi-treated embryos imaged at 5 DPF. Scale bar = 1 mm. Animals were treated with epinephrine prior to imaging. (**D**) Quantification of dorsal melanocytes per animal in 5 DPF wild-type, *gdf6a(lf)* mutant, vehicle-, and BMPi-treated embryos. n = 11, 9, 11, and 15 embryos, respectively, from two independent experiments (N = 2). (**E**) Expression of melanocyte differentiation markers *mc1r, tyr,* and *tyrp1b* by qRT-PCR in wild-type, *gdf6a(lf)* mutant, vehicle-, and BMPi-treated embryos. n = 5–6 replicates across two independent experiments (N = 2) for each group. Expression was normalized to *β-actin*. Error bars represent mean + /- SEM. P-values were calculated using Student's t-test in panel B and E, and one-way ANOVA with Tukey's multiple comparisons test in panels D, *p<0.05, **p<0.01, ***p<0.001, ****p<0.0001, n.s., not significant.

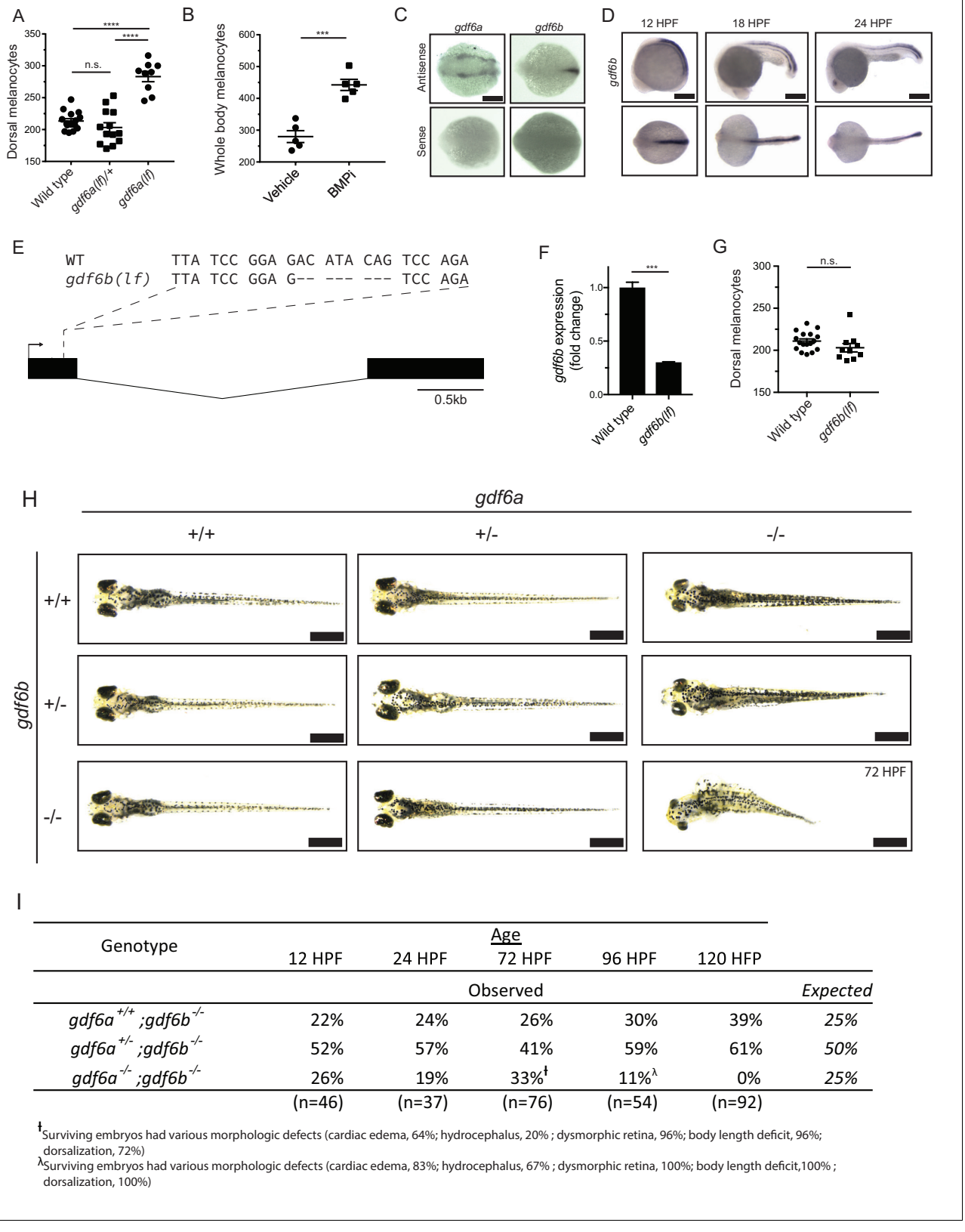

I

Genotype	Age 12 HPF	24 HPF	72 HPF	96 HPF	120 HFP	
			Observed			*Expected*
gdf6a$^{+/+}$;*gdf6b*$^{-/-}$	22%	24%	26%	30%	39%	*25%*
gdf6a$^{+/-}$;*gdf6b*$^{-/-}$	52%	57%	41%	59%	61%	*50%*
gdf6a$^{-/-}$;*gdf6b*$^{-/-}$	26%	19%	33%†	11%$^{\lambda}$	0%	*25%*
	(n=46)	(n=37)	(n=76)	(n=54)	(n=92)	

†Surviving embryos had various morphologic defects (cardiac edema, 64%; hydrocephalus, 20% ; dysmorphic retina, 96%; body length deficit, 96%; dorsalization, 72%)

$^{\lambda}$Surviving embryos had various morphologic defects (cardiac edema, 83%; hydrocephalus, 67% ; dysmorphic retina, 100%; body length deficit,100% ; dorsalization, 100%)

Figure 1—figure supplement 1. *gdf6* paralogs are necessary for normal embryonic development. (**A**) Quantification of dorsal melanocytes in *gdf6a(lf/+)* heterozygotes, *gdf6a(lf)* homozygotes and wild-type embryos. (**B**) Quantification of whole-body melanocytes in vehicle- and BMPi-treated embryos.

Figure 1—figure supplement 1 continued on next page

Figure 1—figure supplement 1 continued

(**C**) Verification of *gdf6a* and *gdf6b* probe specificity. (**D**) RNA in situ hybridization for *gdf6b* at 12-, 18-, and 24 hr post-fertilization, scale bar = 500 μm. (**E**) Sequence of *gdf6b(lf)* mutant indicating deletion and frameshift in exon 1. (**F**) Decreased *gdf6b* expression in *gdf6b(lf)* embryos. (**G**) Quantification of dorsal melanocytes in *gdf6b(lf)* mutants compared to wild-type embryos. (**H**) Images of *gdf6a(lf)* and *gdf6b(lf)* mutant combinations. *gdf6b(lf)* animals have no morphologic defects compared to wild-type embryos at 5 DPF, while *gdf6a(lf)* animals show pigmentation and eye morphology defects. *gdf6a(lf);gdf6b(lf)* double mutants show significant morphologic defects associated with *gdf6a(lf)* as well as decreased body length, cardiac edema and hydrocephalus. Scale bar = 1 mm. (**I**) Survival of *gdf6b(lf)* embryos with *gdf6a(lf)* mutations. †, surviving embryos had various morphologic defects (cardiac edema, 63%; hydrocephalus, 21%; dysmorphic retina, 96%; body length deficit, 96%; dorsalization, 71%). λ, surviving embryos had various morphologic defects (cardiac edema, 83%; hydrocephalus, 67%; dysmorphic retina, 100%; body length deficit, 100%; dorsalization, 100%). Error bars represent mean + /- SEM. P-values were calculated using one-way ANOVA with Tukey's multiple comparison test for panel A and with Student's t-test for panels B, F, and G. ***p<0.001, ****p<0.0001, n.s., not significant.

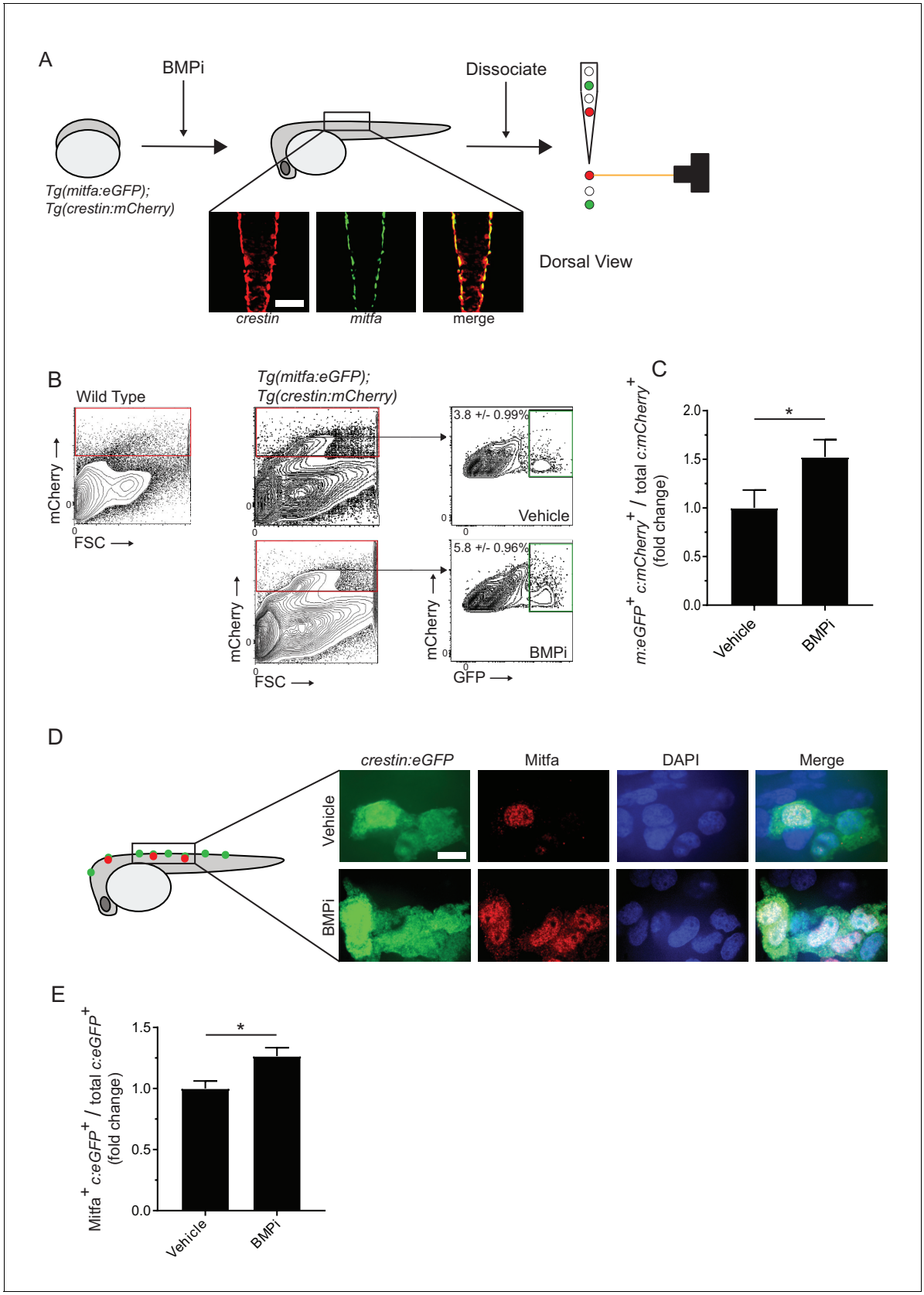

Figure 2. Inhibition of BMP signaling increases *mitfa*-positive neural crest cells. (**A**) Diagram of experiment. *Tg(crestin:mCherry); Tg(mitfa:eGFP)* embryos were treated with BMPi from 12 to 24 HPF. At 24 HPF, embryos were dissociated and analyzed via flow cytometry for GFP- and mCherry-

Figure 2 continued on next page

Figure 2 continued

positive cells, scale bar = 200 μm. (**B**) Gating strategy based on non-transgenic wild-type control to identify *crestin:mCherry*-positive cells and *crestin:mCherry/mitfa:eGFP* double-positive cells. Top, control vehicle-treated embryos. Bottom, BMPi-treated embryos. (**C**) Fold change in *crestin:mCherry/mitfa:eGFP* double-positive cells per total *crestin:mCherry*-positive cells in vehicle and BMPi-treated groups, N = 3 biological replicates of 80–100 stage-matched embryos pooled for each condition. *m:eGFP, mitfa:eGFP; c:mCherry, crestin:mCherry.* (**D**) anti-Mitfa immunofluorescence in *Tg(crestin:eGFP)* embryos treated with BMPi or vehicle control and fixed at 24 hr, scaled bar = 10 μm. (**E**) Fold change in Mitfa/*crestin:eGFP* double-positive cells per total *crestin:eGFP*-cells, n = 16 embryos from two independent experiments (N = 2) for each condition. *c:eGFP, crestin:eGFP.* Error bars represent mean + /- SEM; P-value was calculated using ratio-paired t-test in panel C and Student's t-test in panel E, *p<0.05.

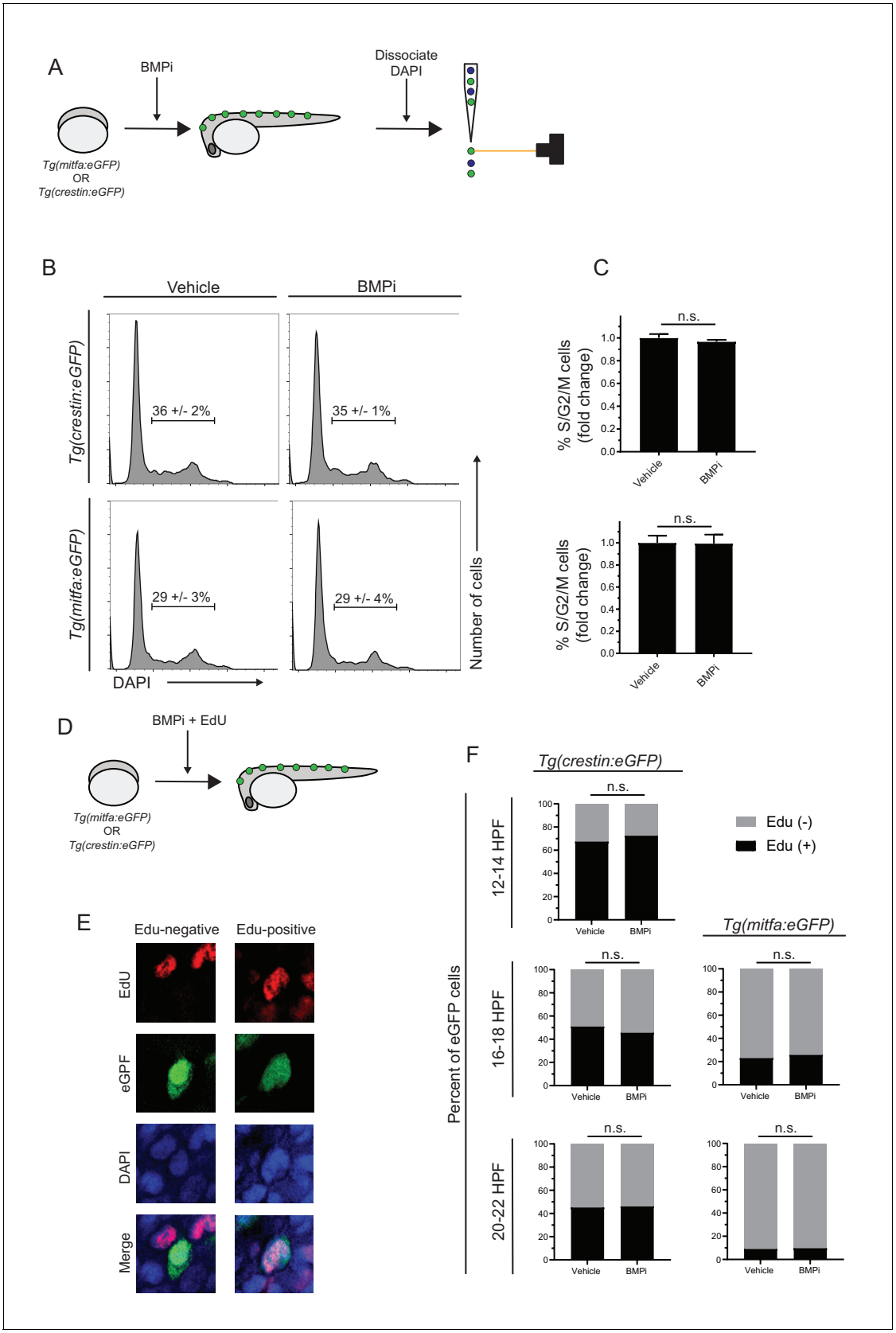

Figure 2—figure supplement 1. Increased proliferation is not observed in neural crest and pigment progenitor cell populations of BMPi-treated embryos. (**A**) Diagram of experiment. Embryos expressing either *Tg(mitfa:eGFP)* or *Tg(crestin:eGFP)* were treated with BMP inhibitor from 12 to 24 HPF.

Figure 2—figure supplement 1 continued on next page

Figure 2—figure supplement 1 continued

Following treatment, embryos were dissociated, fixed, and stained for DNA content using DAPI and analyzed via flow cytometry. Scale bar = 200 μm. (**B**) Flow cytometry histograms showing the percentage of cells in S/G2/M phases in *crestin:eGFP*-positive or *Tg(mitfa:eGFP*-positive cell populations in BMPi-treated embryos compared to vehicle-treated embryos. (**C**) Fold change of *crestin:eGFP*-positive cells (top) and *mitfa:eGFP*-positive cells (bottom) in S/G2/M phases. n = 3 biological replicates of 80–100 stage-matched embryos pooled for each condition. (**D**) Diagram of experiment. Embryos expressing either *Tg(mitfa:eGFP)* or *Tg(crestin:eGFP)* were treated with BMP inhibitor starting at 12 HPF. Embryos were concurrently treated with EdU from 12 to 14 HPF, 16–18 HPF, or 20–22 HPF. Following EdU treatment, embryos were fixed and assess for EdU incorporation. (**E**) Example image of EdU incorporation in eGFP-positive cells in vehicle- and BMPi-treated embryos. (**F**) Quantification of EdU incorporation in *Tg(crestin:eGFP)* and *Tg (mitfa:eGFP)* embryos at different time points, n = 62–166 eGFP-positive cells from two independent experiments (N = 2) for each condition and time point. Error bars represent mean + /- SEM, P-values were calculated using ratio paired t-test for panel C and Fisher's exact test for panel F, n.s., not significant.

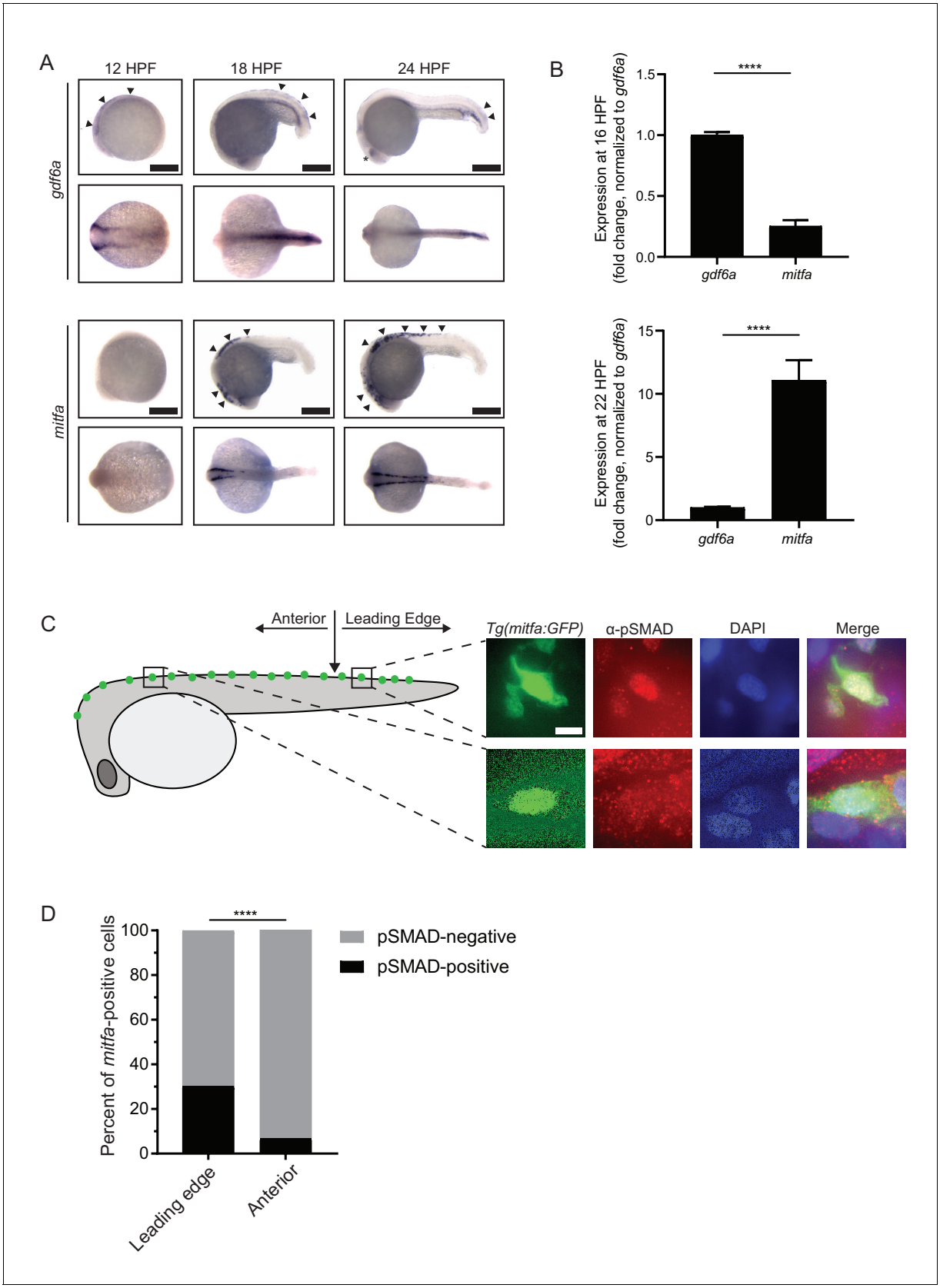

Figure 3. *gdf6a* expression and BMP activity in pigment progenitor cells. (**A**) RNA in situ hybridization for *gdf6a* (top) and *mitfa* (bottom) at 12-, 18-, and 24 hr post-fertilization. Arrowheads indicate expression domains in the region of the neural crest of *gdf6a* and *mitfa*. Asterisk indicates known dorsal

Figure 3 continued on next page

Figure 3 continued

retinal expression of *gdf6a*. Scale bar = 500 μm. (**B**) Expression of *gdf6a* and *mitfa* from neural crest cells isolated from *Tg(crestin:eGFP)* embryos by FACS at 16 HPF and 22 HPF. Samples were normalized to *gdf6a* expression. n = 5–6 replicates per conditions from two independent experiments (N = 2). (**C**) Images of GFP-positive cells from *Tg(mitfa:eGFP)* zebrafish stained with α-pSMAD 1/5/8 antibody. Scale bar = 10 μm. (**D**) Quantification of *mitfa:eGFP*-positive cells that are phospho-SMAD1/5/8-positive. The leading edge encompassed the five most posterior *mitfa*-positive cells, whereas anterior cells constituted any *mitfa*-positive cells anterior to the leading edge. n = 102 and 186 for distal leading edge and anterior cells, respectively, from three independent experiments (N = 3). P-values were calculated using Fisher's exact test for panels B and D, ****p<0.0001.

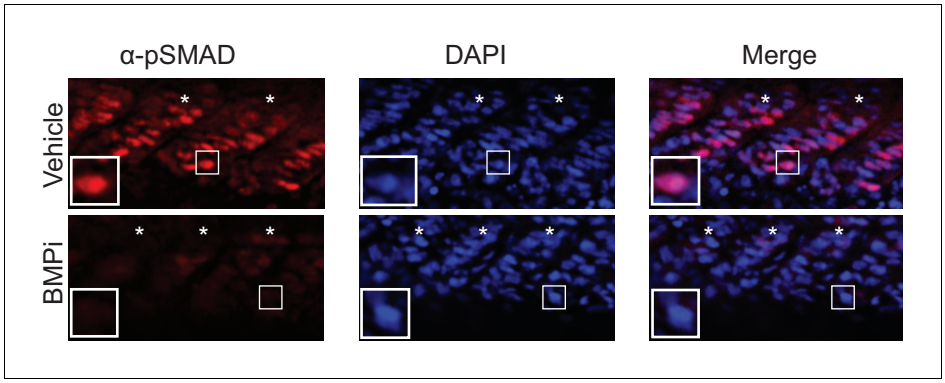

Figure 3—figure supplement 1. Treatment with the BMP inhibitor DMH1 reduces phospho-SMAD1/5/8 staining in embryos Top, vehicle-treated animals and, bottom, BMPi-treated animals showing lateral views of developing muscle segments, identified by asterisks. Insets show individual nuclei. Photomicrographs for pSMAD-1/5/8-stained embryos were taken at the same exposure settings.

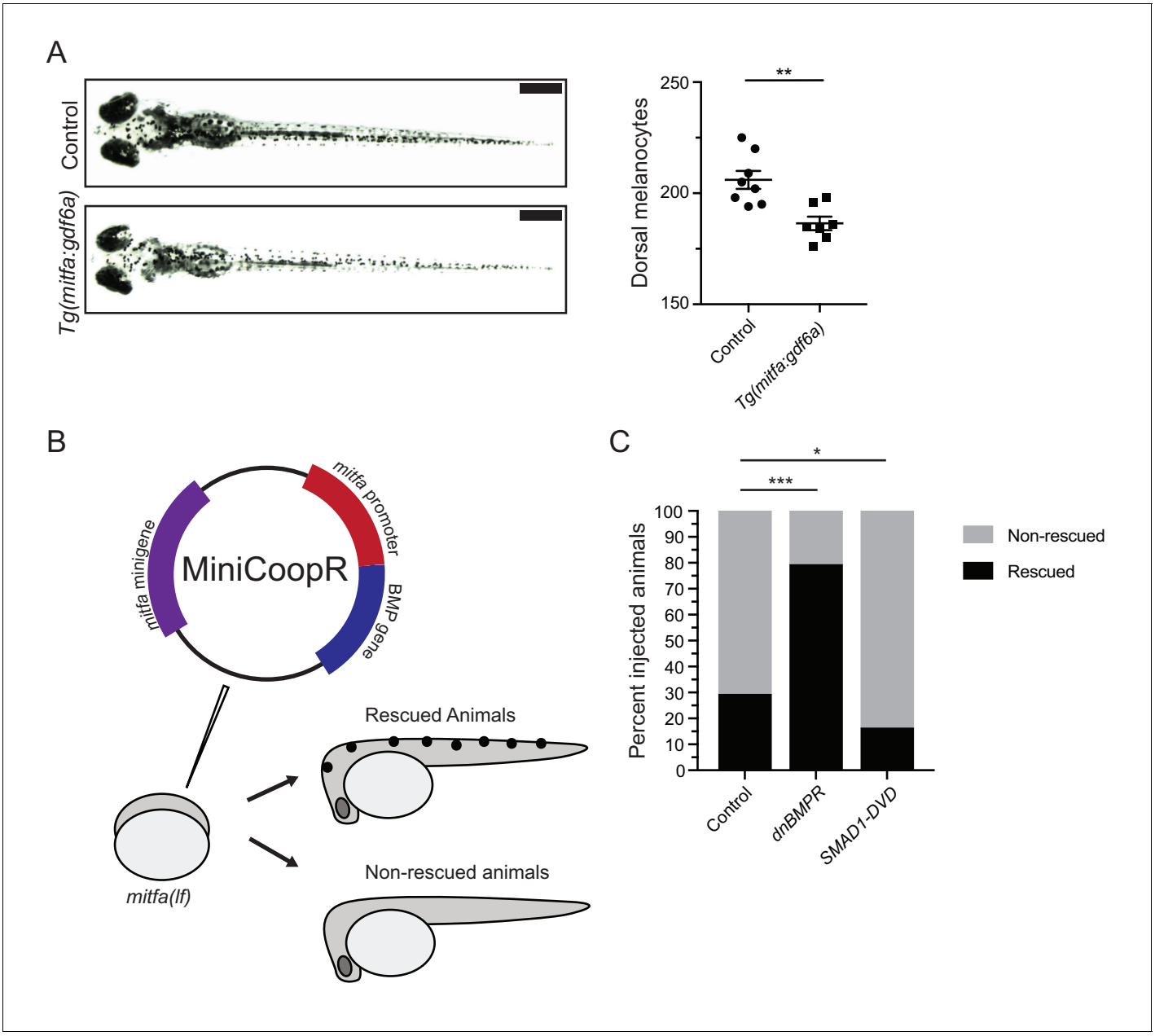

Figure 4. BMP signaling within pigment progenitor cells can impact embryonic melanocytes. (**A**) *Tg(mitfa:gdf6a)* and non-transgenic sibling control embryos (left), and quantification of dorsal melanocytes per animal in each group (right). Animals were treated with epinephrine prior to imaging at 5 DPF, n = 8 and 7 for control and *Tg(mitfa:gdf6a)* groups, respectively, from two independent experiments (N = 2). Scale bar = 1 mm. (**B**) Diagram of miniCoopR rescue experiment. Animals harboring a *mitfa(lf)* mutation were injected at the single-cell stage with the miniCoopR vector containing a BMP gene. Animals were evaluated at 5 DPF for the presence of melanocytes. If melanocytes were present, that animal was scored as rescued, whereas animals lacking melanocytes were scored as non-rescued. (**C**) Percentages of rescued and non-rescued animals following injection of a miniCoopR-BMP vector, n = 361, 193 and 152 for control, *dnBMPR*, and *SMAD1-DVD* groups, respectively, from four independent experiments (N = 4). Error bars represent mean + /- SEM. P-values were calculated Student's t-test for panel A and with Fisher's exact test with Bonferroni's correction for panel C, *p<0.05, **p<0.01, ***p<0.001.

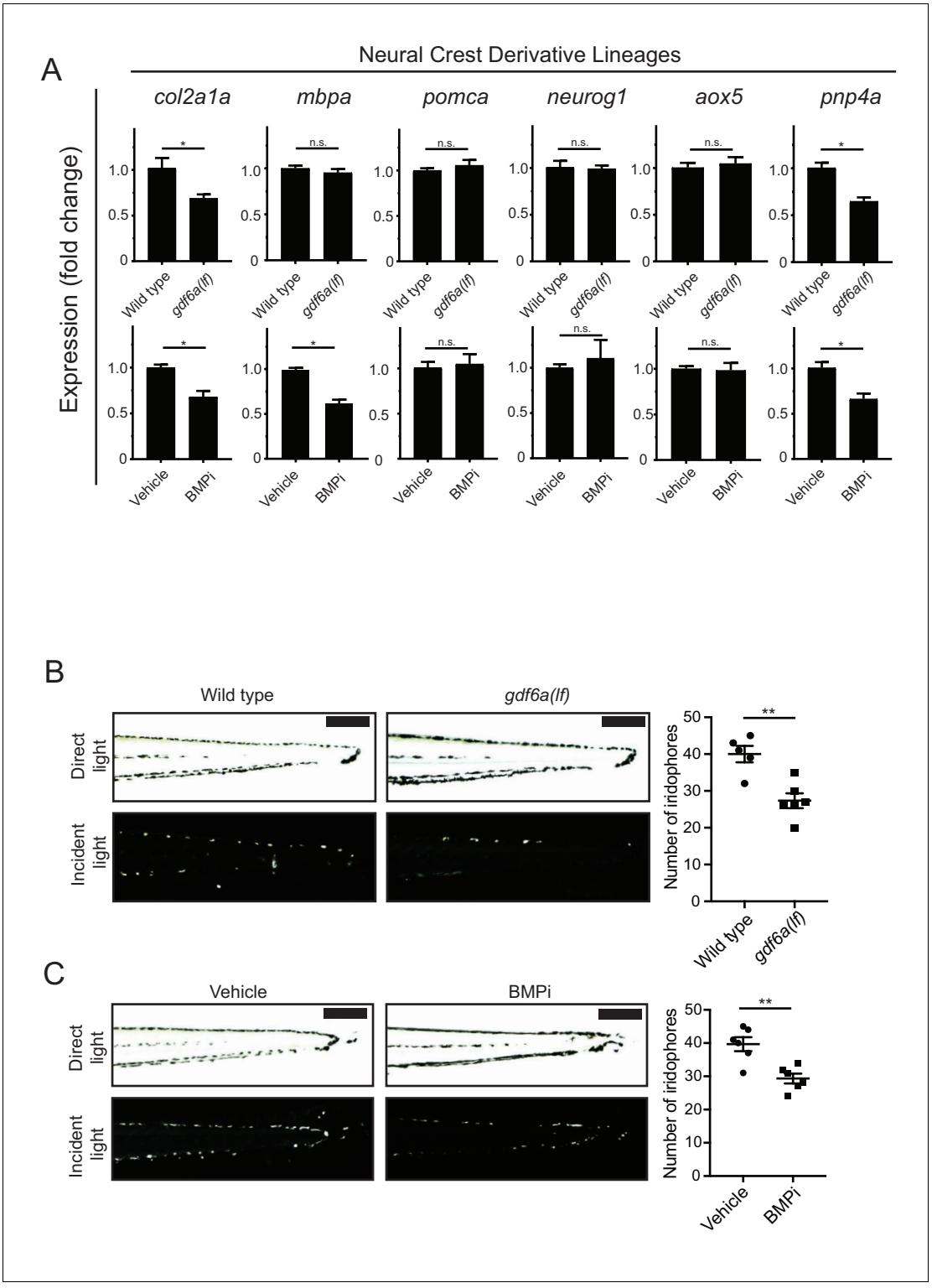

Figure 5. *gdf6a* loss and BMP inhibition impact development of specific neural crest derivatives. (**A**) Expression analyses of multiple neural crest and neural crest derivative lineage markers. qRT-PCR was used to assess changes in markers of neural crest markers and neural crest derivatives in *gdf6a(lf)* embryonic zebrafish (top) and BMPi-treated wild-type zebrafish (bottom) at 5 DPF; *col2a1a*, chondrocytes; *mbpa*, glial; *pomca*, adrenal medullary cells; *neurog1*, neuronal cells; *aox5*, xanthophores; *pnp4a*, iridophores; n = 5–6 for each group from two independent experiments (N = 2). (**B**) Direct light (top) and incident light (bottom) images of wild-type and *gdf6a(lf)* embryos at 5 DPF and quantification of dorsal iridophores (right) per animal in each group. Animals were treated with epinephrine prior to imaging at 5 DPF; n = 5 and 6 for wild-type and *gdf6a(lf)* groups, respectively, from two

Figure 5 continued on next page

Figure 5 continued

independent experiments (N = 2); scale bar = 500 μm. (**C**) Direct light, top, and incident light, bottom, images of wild-type embryos treated with vehicle or BMPi from 12 to 24 HPF and quantification of dorsal iridophores, right, per animal in vehicle and BMPi treated groups. Animals treated with epinephrine prior to imaging at 5 DPF, n = 6 and 6 for vehicle and BMPi groups, respectively, from two independent experiments (N = 2); scale bar = 1 mm. Error bars represent mean + /- SEM, P-values calculated with Student's t-test, *p<0.05, **p<0.01, n.s., not significant.

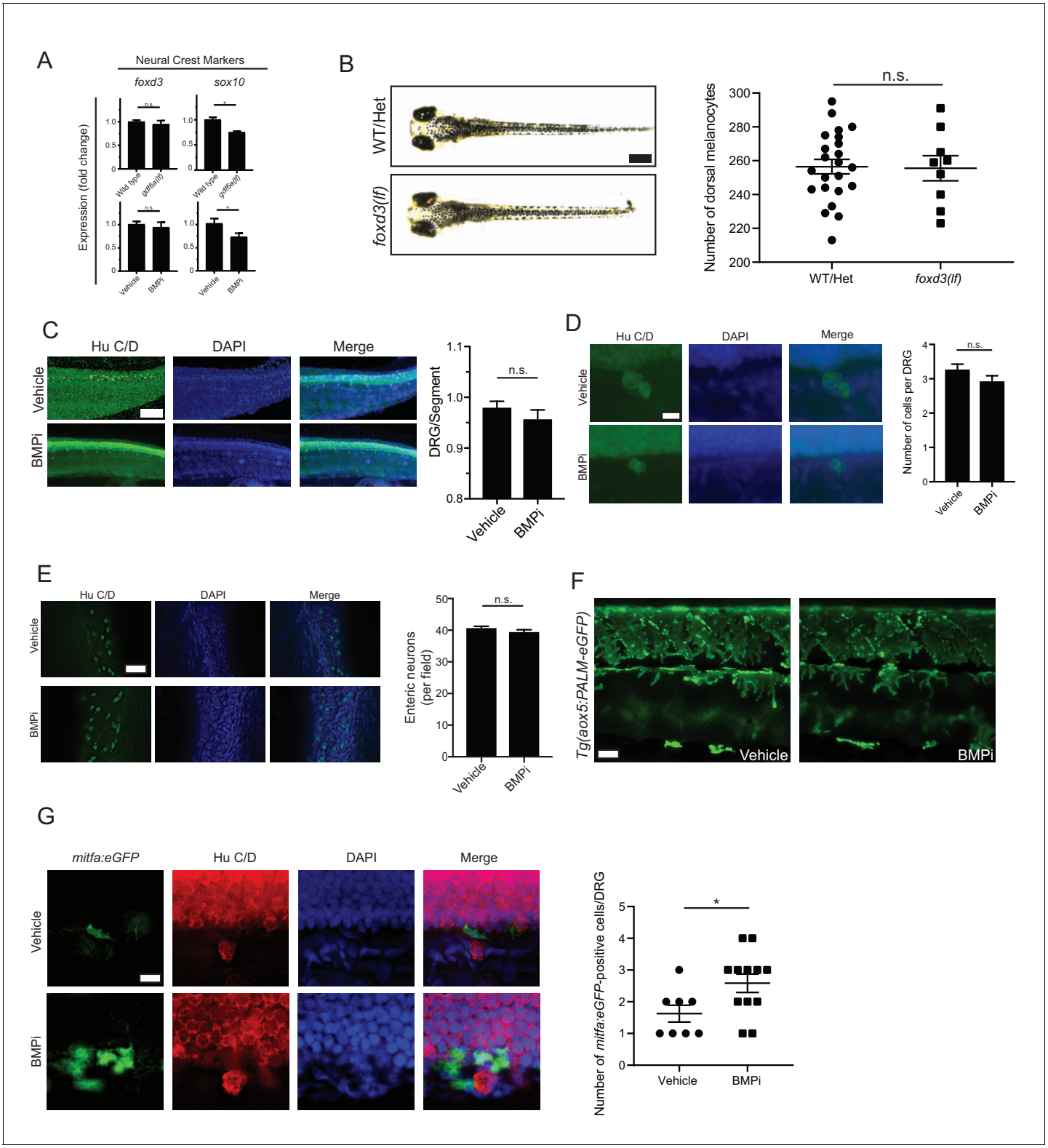

Figure 5—figure supplement 1. Neural crest cells and derivative populations show variable response to BMP inhibition. (**A**) Expression analyses of neural crest markers *foxd3* and *sox10* by qRT-PCR in *gdf6a(lf)* and BMPi-treated animals compared to controls, n = 4–6 replicates for each condition from two independent experiments (N = 2). (**B**) Left, photomicrographs of wild-type/*foxp3(lf)* heterozygous and *foxd3(lf)* homozygous embryos under BMPi treatment compared to controls, and, right, melanocyte quantification in these embryos, n = 23 and 9 control and *foxd3(lf)* embryos, respectively, from two independent experiments (N = 2). (**C**) Left, Hu C/D staining for dorsal root ganglion structures and, right, quantification of dorsal root ganglia

Figure 5—figure supplement 1 continued on next page

Figure 5—figure supplement 1 continued

developing per segment, n = 5 per group. Scale bar = 50 μm. (**D**) Left, photomicrographs of individual Hu C/D-stained DRG's and, right, quantification in the number of cells populating each individual DRG; n = 30 per group. Scale bar = 10 μm. (**E**) Left, Hu C/D staining for enteric neurons and, right, quantification of the number of enteric neurons per field in developing gastrointestinal tract; n = 5 per group. Scale bar = 50 μm. (**F**) Qualitative evaluation of xanthophore development using *Tg(aox5:PALM-eGFP)* embryos treated with vehicle or BMPi showed no apparent change in density or localization of xanthophores between vehicle- and BMPi-treated embryos, supported by no change in *aox5* expression as shown in ***Figure 5A***. (**G**) Left, Hu C/D staining of vehicle- and BMPi-treated *Tg(mitfa:eGFP)* embryos and, right, quantification of *mitfa:eGFP*-positive, DRG-associated cells in control and BMPi-treated groups, n = 8 and 12 DRG's evaluated in vehicle- and BMPi-treated embryos, respectively, from two independent experiments (N = 2). Error bars represent mean + /- SEM. P-values were calculated using Student's t-test, *p<0.05, n.s., not significant.

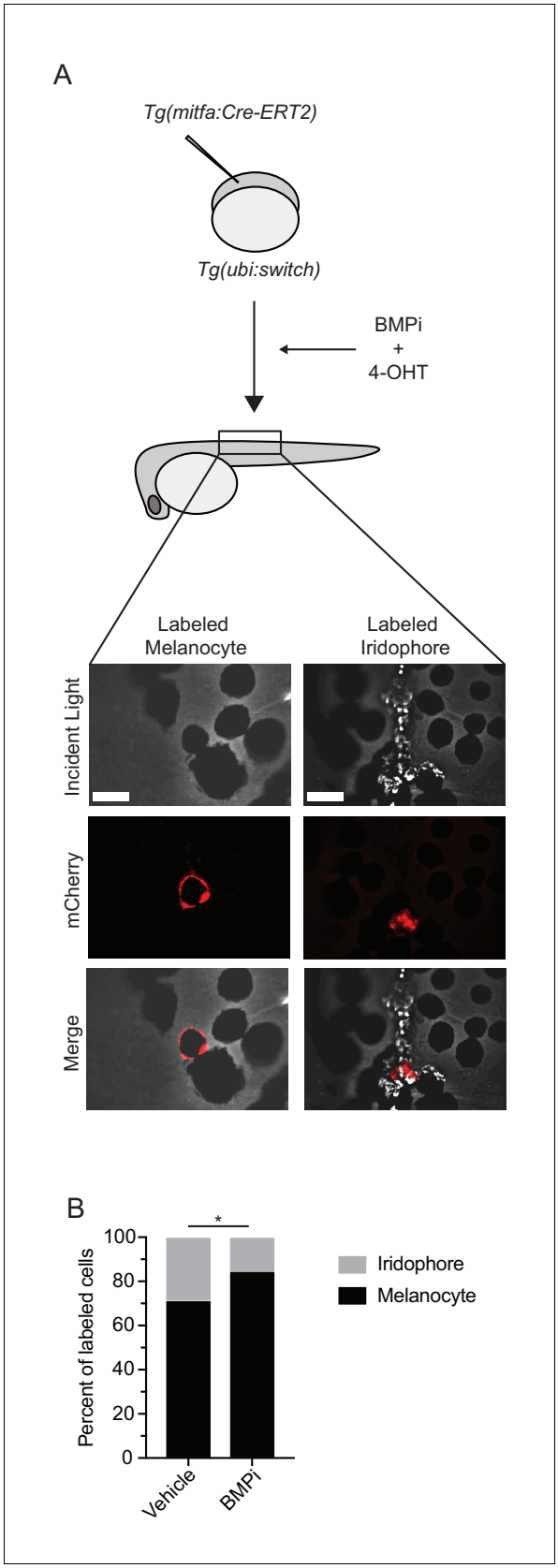

Figure 6. BMP inhibition impacts fate specification of *mitfa*-positive pigment progenitor cells. (**A**) Diagram of lineage tracing experiment. Embryos containing *Tg(ubi:switch)* were injected with a *mitfa:Cre-ERT2* construct and

Figure 6 continued on next page

Figure 6 continued

treated with BMPi and tamoxifen (4-OHT) from 12 to 24 HPF to block BMP signaling and allow Cre recombination. At 5 DPF, animals were screened for successful recombination by presence of single mCherry-labeled pigment cells, and the identities of those cells were assessed using incident light. Scale bar = 40 μm. (**B**) Quantification of mCherry-labeled cell fates at 5 DPF in vehicle and BMPi-treated animals, n = 101 and 80 labeled cells for vehicle and BMPi groups, respectively, from five independent experiments (N = 5); P-value calculated using Fisher's exact test, *p<0.05.

	Mel.	Irid.	
Veh.	71	30	101
BMPi	67	13	80
	138	43	181

$p < 0.05$

Figure 6—figure supplement 1. Quantification of iridophore and melanocyte numbers from lineage tracing
Number of iridophores and melanocytes identified by lineage tracing under each condition. P-value was calculated using Fisher's exact test, $p<0.05$.

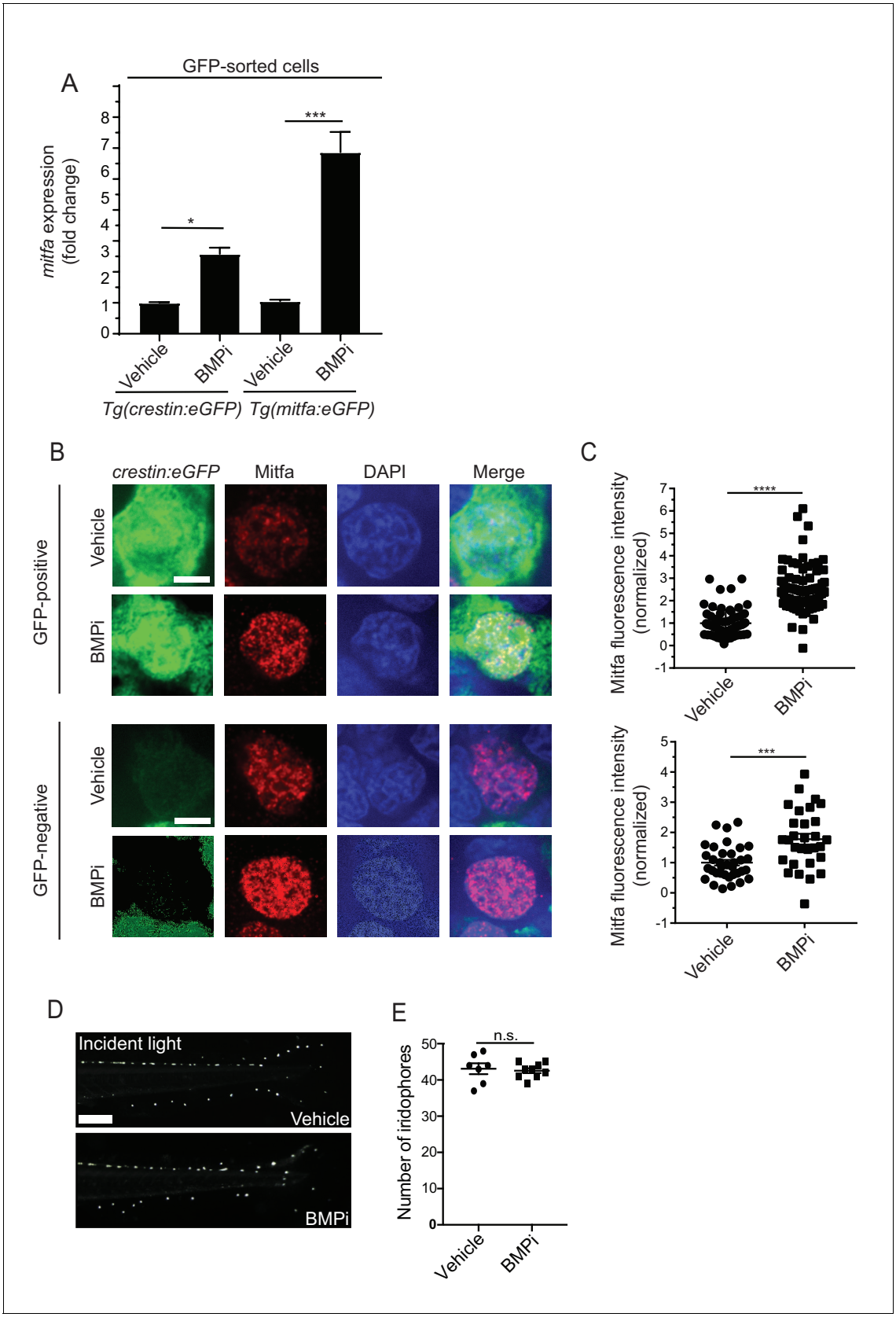

Figure 7. BMP signaling regulates expression of and acts through *mitfa* to impact pigment cell fates. (**A**) *mitfa* expression in sorted GFP-positive cells from *Tg(crestin:eGFP)* and *Tg(mitfa:eGFP)* embryos treated with vehicle or BMPi from 12 to 24 HPF, n = 4–5 replicates for each condition from two

Figure 7 continued on next page

Figure 7 continued

independent experiments (N = 2). (**B**) anti-Mitfa immunofluorescence, DAPI and merged images of *Tg(crestin:eGFP)* embryos treated with vehicle control or BMPi in GFP-positive cells (top) and GFP-negative cells (bottom), scale bar = 5 μm. (**C**) Quantification of anti-Mitfa fluorescence intensity of individual nuclei in GFP-positive cells (top) and GFP-negative cells (bottom); n = 65 and 74 for GFP-positive vehicle and BMPi groups, respectively; n = 35 and 30 for GFP-negative vehicle and BMPi groups, respectively, from three independent experiments (N = 3). (**D**) Incident light images of *mitfa (lf)* embryonic zebrafish treated with vehicle or BMPi from 12 to 24 HPF and imaged at 5 DPF, scale bar = 1 mm. (**E**) Quantification of dorsal iridophores in *mitfa(lf)* embryonic zebrafish treated with vehicle or BMPi from 12 to 24 HPF, n = 7 and 9 for vehicle and BMPi groups, respectively, from two independent experiments (N = 2). Error bars represent mean + /- SEM, P-value was calculated using one-way ANOVA with Tukey's multiple comparisons test in panel A and Student's t-test in panel C and E. *p<0.05, ***p<0.001, ****p<0.0001, n.s., not significant.

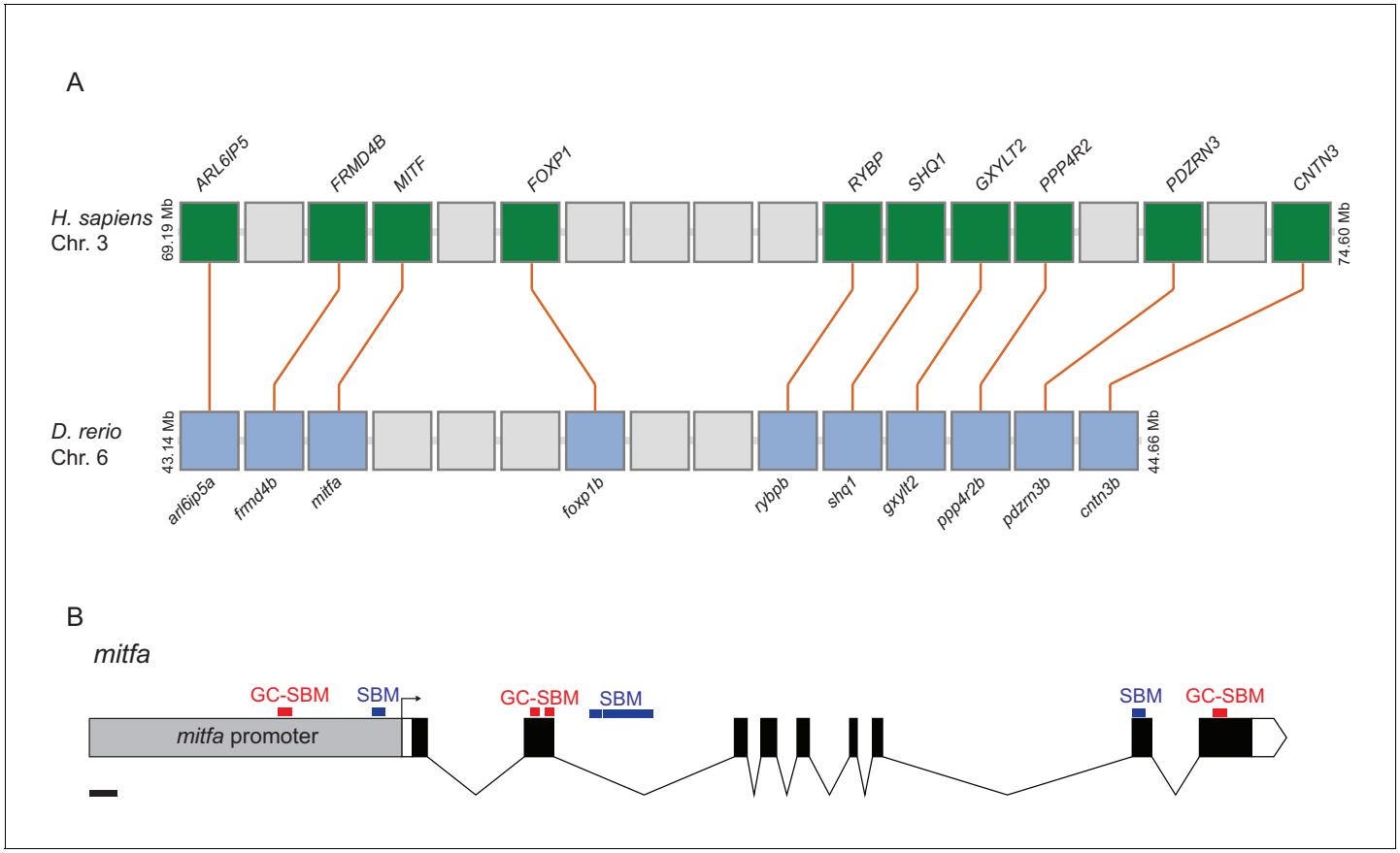

Figure 7—figure supplement 1. Diagram of synteny between *MITF* and *mitfa* loci and SMAD binding motifs at the *mitfa* locus. (**A**) Diagram of orthologous genes flanking the *MITF* and *mitfa* loci in human and zebrafish genomes, respectively. *H. sapiens, Homo sapiens; D. rerio, Danio rerio.* (**B**) Diagram of *mitfa* locus, including promoter, intronic and exonic regions with identified SMAD binding motifs (SBM) and GC-rich SMAD binding motifs (GC-SBM). Scale bar = 200 bp.